Characterization of Iron Oxide Nanoparticles in an Fe_2O_3−SiO_2 Composite Prepared by a Sol−Gel Method

G. Ennas, A. Musinu, G. Piccaluga,* and D. Zedda

Dipartimento di Scienze Chimiche, Universita', Via Ospedale, 72, 09124 Cagliari, Italy

D. Gatteschi, C. Sangregorio, and J. L. Stanger

Dipartimento di Chimica, Universita', Via Maragliano 75, 50144, Firenze, Italy

G. Concas and G. Spano

Dipartimento di Scienze Fisiche, Universita', Via Ospedale, 72, 09124 Cagliari, Italy

Received June 2, 1997. Revised Manuscript Received November 25, 1997

An Fe_2O_3−SiO_2 composite was prepared by a gelation method that adopts tetraethoxysilane and iron(III) nitrate as starting materials. The dried gel was treated at increasing temperatures, and the samples were characterized by XRD, TEM, magnetic susceptibility measurements, and EPR and Mössbauer spectroscopies. Nanometer size (3−4 nm) X-ray-amorphous iron(III) oxide particles are observed in the samples treated at low temperature. These particles display superparamagnetic behavior in the Mössbauer spectra and susceptibility measurements, and their magnetic moments indicate antiferromagnetic clustering. The occurrence of two sites for iron ions, one in the bulk and one on the surface of nanoparticles, is suggested by EPR and Mössbauer spectroscopies. Heating of the samples to higher temperatures (T > 700 °C) gives rise to a small increase of the particle size. Simultaneously XRD and TEM exhibit the formation of γ-Fe_2O_3 crystalline particles, Mössbauer spectra reveal a large change in the magnetization, magnetic measurements show the transition from antiferro- to ferrimagnetic behavior, and the signals of ferrimagnetic resonance appear in the EPR spectra. Superparamagnetic relaxation in these particles was investigated by ac susceptibility measurements and paramagnetic resonance experiments at variable temperatures. Further increase in temperature gives rise to the formation of α-Fe_2O_3. Atomic reorganization processes taking place during these transitions are discussed.

Introduction

The dependence of physical properties of materials on grain size is a well-known phenomenon.[1] The interest in this field is increased on account of the observation that materials with nanometer-size particles (1−10 nm in diameter) exhibit novel electronic, optical, magnetic, and chemical properties, and many efforts have been made to set up new appropriate preparation methods.[2−4] γ-Fe_2O_3 (maghemite) has received much attention in this connection because of its magnetic and catalytic applications.

A critical obstacle in assembling and maintaining a nanoscale material is its tendency to aggregate.[5] A further problem for pure maghemite comes from its conversion into α-Fe_2O_3 (hematite) at rather low temperature (∼300 °C).[6] Both to avoid sintering and to stabilize the maghemite phase, nanocomposites have been prepared in which γ-Fe_2O_3 is incorporated into a polymer, a glass, or a ceramic.

To this end, several preparation methods have been used. For instance, Ziolo et al.[5] exchanged a sulfonated polystyrene resin with an aqueous solution of iron(II) chloride and obtained the γ-Fe_2O_3 phase through exposure of the exchanged resin to 12.5 M NaOH and addition of dilute aqueous H_2O_2. Alternatively, Chanéac et al.[6] first prepared colloidal magnetite by adding a mixture of $FeCl_2$ and $FeCl_3$ to a base and then converted the precipitate of magnetite into γ-Fe_2O_3 by treatment with $HClO_4$. γ-Fe_2O_3 was either dispersed in poly(vinyl alcohol) or covered by silica formed by gelling a triethoxysilane solution. Silica-supported maghemite was also prepared by adding to a silica gel an aqueous $Fe(NO_3)_3$ solution by incipient wetness.[7]

Sol−gel methods, which have been found to be effective for dispersing small metal and oxide particles in nonmetallic matrixes,[8−10] were also proposed for the

* To whom correspondence should be addressed: Prof. Giorgio Piccaluga, Tel +3970-6758608; FAX +3970-6758605, Dipartimento di Scienze Chimiche, Universita', Via Ospedale, 72, 09124 Cagliari, Italy.

(1) Smith, W. F. *Principles of Materials Science Engineering*; McGraw Hill Book Company: Singapore, 1986.
(2) Birringer, R. *Mater. Sci. Eng.* **1989**, *A117*, 32.
(3) Gleiter, H. *J. Appl. Crystallogr.* **1991**, *24*, 79.
(4) Siegel, R. W. *Nanostruct. Mater.* **1993**, *3*, 1.
(5) Ziolo, R. F.; Giannelis, E. P.; Weinstein, B. A.; O'Horo, M. P.; Ganguly, B. N.; Mehrotra, V.; Russel M. W.; Huffman, D. R. *Science* **1992**, *257*, 219.
(6) Chanéac, C.; Tronc E.; Jolivet, J. P. *Nanostruct. Mater.* **1995**, *6*, 715.
(7) (7) Lund, C. R. F.; Dumesic, J. A. *J. Phys. Chem.* **1981**, *85*, 3075.
(8) Roy R. A.; Roy, R. *Mater. Res. Bull.* **1984**, *19*, 169.

S0897-4756(97)00400-6 CCC: $15.00
Published on Web 01/27/1998

preparation of $Fe_2O_3-SiO_2$ composites. Guglielmi and Principi[11] used $Si(OC_2H_5)_4$ (TEOS) and $Fe(OC_2H_5)_3$ in alcoholic solution as gelling precursors. The gels were dried and heated in the temperature range 40−1000 °C; the samples gave X-ray-amorphous patterns up to 700 °C, while heating to higher temperature yielded the formation of α-Fe_2O_3. Very similar results were obtained by Tanaka et al.,[12] who used TEOS and iron(III) acetylacetonate as starting reagents. Ida et al.[13] prepared the gels by hydrolysis of a mixed solution of TEOS and iron (III) nitrate dissolved in ethylene glycol; subsequent calcination gave rise to the formation of γ-Fe_2O_3 particles, which convert to α-Fe_2O_3 at temperatures higher than 650 °C.

The present paper reports the preparation of an $Fe_2O_3-SiO_2$ nanocomposite by a very simple sol−gel method, recently proposed for the synthesis of $Me-SiO_2$ systems.[14−16] Commercial precursors (TEOS and iron(III) nitrate) were dissolved in an alcoholic aqueous medium, and the gels formed after a few days were heated giving the final materials without further manipulation. Since the decomposition of the iron salt can lead to the formation of various forms of oxides with different properties, special attention was devoted to the characterization of the material obtained under the adopted experimental conditions and after treatments at elevated temperatures. The amorphous and crystalline nature of the products, the occurrence of recognizable phases, and the size of the particles were controlled by X-ray diffraction (XRD) and transmission electron microscopy (TEM); the local order around Fe(III) ions was investigated by electron paramagnetic resonance (EPR), ferrimagnetic resonance (FIMR), and Mössbauer spectroscopy. The magnetic properties were monitored both by ac and dc magnetic susceptibility measurements.

Experimental Section

A composite of iron oxide and silica with ratio $Fe_2O_3/(Fe_2O_3 + SiO_2)$ equal to 7.1 mol % (16.9 wt %) was prepared by mixing an alcoholic solution of TEOS (Aldrich 98%) and an aqueous solution of iron nitrate ($Fe(NO_3)_3 \cdot 9H_2O$, Aldrich 98%). Several compositions were experimented with in order to obtain a clear sol in the first stage of preparation, which led to the choice of a molar ratio of ethyl alcohol to TEOS to water equal to 3.85:1:10.2.

After 1 h of stirring, the pH of the mixture was 0.9. The clear sol was then poured into a Teflon beaker and allowed to gel in air. The high acidity prevents the precipitation of iron hydroxides, though it leads to a relatively long gelation time. In fact, a gelation time of 9 days resulted for the several preparations that were carried out.

The gel was dried in an oven by slowly raising the temperature to 100 °C over a week. Thermogravimetric analysis (TGA), carried out in air on the dried gel, showed that the weight loss due to residual water elimination and nitrate decomposition is completed at about 180 °C. On this basis, to avoid the formation of the α-Fe_2O_3 phase, the dried sample was powdered and kept for 24 h at 150 °C. The sample was then rised to higher temperatures, with steps of 50 °C up to 500 °C and of 100 °C up to 1100 °C, and kept for 30 min at each temperature. The labels Fe150, Fe300, and so on, used below, indicate the treatment temperature.

Structural evolution of the samples was monitored by XRD using $\theta-2\theta$ conventional equipment (Siemens D500) with Mo Kα wavelength; iron oxide nanoparticles were observed in electron micrographs obtained with a TEM (JEOL 200CX), operating at 200 kV.

Static magnetic susceptibility was measured with a Metronique Ingeniérie MS02 SQUID magnetometer equipped with a superconducting magnet capable of producing fields up to 8 T. Zero field cooled (ZFC) and field cooled (FC) magnetization data were collected with an applied field of 50 Oe. Ac susceptibility experiments were carried out on a laboratory-assembled susceptometer, based on a mutual inductance bridge working in the frequency range 30−1500 Hz.

EPR experiments were carried out on a Varian E9 spectrometer working at X-band (9.25 GHz) and equipped with an Oxford cryostat, which allows temperature variation from 4 K to room temperature. The sample powders were dispersed in a paraffin matrix to prevent orientation of the crystallites along the Zeeman magnetic field, which was observed in preliminary experiments. Although the dilution in paraffin is not exactly known, the interaction between crystallites seems negligible because of the dilution of the γ-Fe_2O_3 particles in the SiO_2 matrix. High-field EPR (HF-EPR) experiments were performed at the High-Magnetic Field Laboratory in Grenoble (France) with an exciting frequency of 250 GHz and at temperatures between 5 and 100 K.

Mössbauer absorption spectra were obtained in a standard transmission geometry, using a source of ^{57}Co in rhodium (37 MBq). Calibration was performed using a 25 μm thick natural iron foil; the isomer shift values are referred to α-Fe. The measurements were carried out at room temperature on powdered samples kept in a Plexiglas holder. The surface density of the absorbers ranges from 105 to 145 mg/cm^2.

Differential thermal analysis (DTA) of the Fe300 sample was carried out with an apparatus (Linseis L62) with a heating rate of 10 °C/min up to 1000 °C.

Results

XRD and TEM. XRD data from Fe150 to Fe600 do not display diffraction peaks; only the amorphous pattern of vitreous silica is visible (Figure 1). After higher thermal treatments, two broadened peaks appear which are ascribed to γ-Fe_2O_3.[17a] As the temperature increases, the γ-Fe_2O_3 peaks grow and the amorphous background undergoes some modifications, indicating structural rearrangements of the glassy network (matrix), which at 1100 °C lead to the formation of crystobalite. Simultaneously, peaks attributable to the α-Fe_2O_3 phase also appear in the spectrum.[17b] Although the γ-Fe_2O_3 signals can be hardly separated from the amorphous pattern, they clearly point out the presence of very small oxide particles at the limits of XRD observation (3−4 nm).

The occurrence of oxide particles is confirmed by TEM observations (Figures 2 and 3). In TEM micrographs, however, particles embedded into the SiO_2 matrix are visible in all the samples. In Fe150 and Fe300 samples, particles of ∼3 nm are observed with difficulty at 100 000 magnification, while the number of observed

(9) Pope, E. J. A.; Mackenzie, J. *J. Non-Cryst. Solids* **1986**, *87*, 185.
(10) Brinker, C. J.; Scherer, G. W. *Sol Gel Science*; Academic Press: San Diego, 1990.
(11) Guglielmi, M.; Principi, G. *J. Non-Cryst. Solids* **1982**, *48*, 161.
(12) Tanaka, K.; Kamiya, K.; Matsuoka, M.; Yoko, T. *J. Non-Cryst. Solids* **1987**, *94*, 356.
(13) Ida, T.; Tsuiki, H.; Ueno, A.; Tohji, K.; Udagawa, Y.; Iwai, K.; Sano, H. *J. Catal.* **1987**, *106*, 428.
(14) Shull, R. D.; Ritter, J. J.; Shapiro, A. J.; Swartzendruber, L. J.; Bennet, L. H. *J. Appl. Phys.* **1990**, *67*, 4490.
(15) Roy, S.; Chatterjee, A.; Chakravorty, D. *J. Mater. Res.* **1993**, *8*, 689.
(16) Wang, J. P.; Luo, H. L. *J. Appl. Phys.* **1994**, *75*, 7425.
(17) Powder Diffraction File card (a) No. 39−1335 and (b) No. 32−664, International Center for Diffraction Data, Swarthmore, PA.

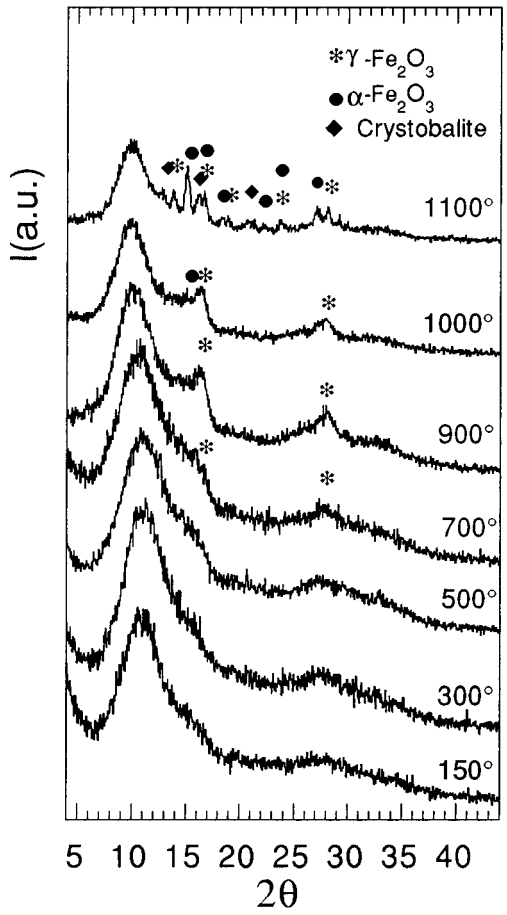

Figure 1. XRD data of the samples heat treated at the reported temperatures.

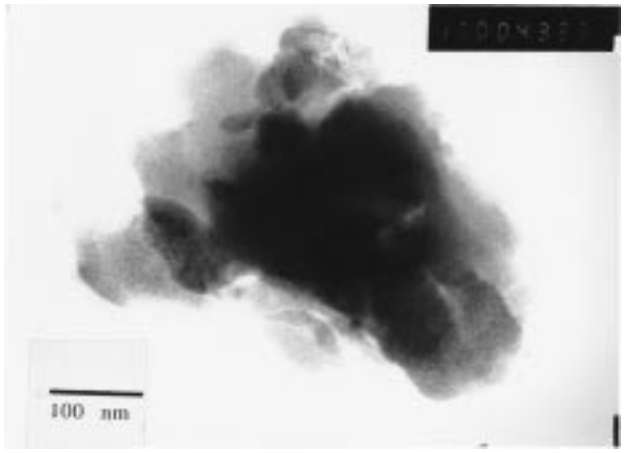

Figure 2. TEM image of the Fe300 sample.

particles increases with temperature and their size at most doubles. In all the cases, a narrow size distribution is obtained, as clearly evident in the reported bright-field micrographs. The dark-field micrographs indicate the amorphous character of the majority of nanoparticles in the samples treated at temperatures lower than 700 °C and their crystallinity at higher temperatures.

TEM observations of the Fe150 sample show the presence of a not negligible amount of impurities (such as unreacted iron nitrate crystals), which disappear at 300 °C. For this reason, only samples treated above this limit will be taken into account.

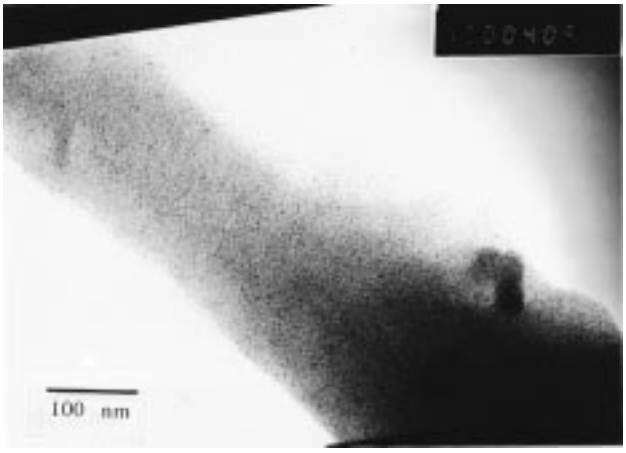

Figure 3. TEM image of the Fe900 sample.

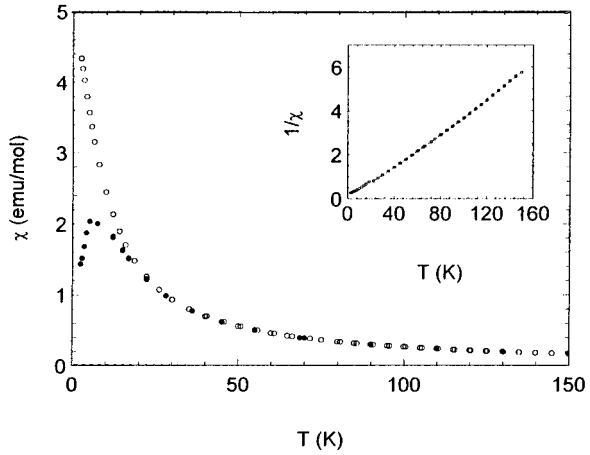

Figure 4. ZFC (full circles) and FC (open circles) magnetization measured as a function of temperature for the Fe900 sample. In the inset is shown the temperature dependence of the inverse susceptibility.

Magnetic Measurements. The ZFC and FC susceptibilities of Fe900 are shown in Figure 4. The results are representative of the behavior of all the samples. At high temperature the two curves coincide and the susceptibility follows a Curie−Weiss law, as shown in the inset of Figure 4, while at lower temperature they start to separate and the ZFC magnetization shows a broad maximum. Such behavior is characteristic of superparamagnetism[18] and is due to the progressive blocking of the magnetization of smaller and smaller particles when temperature is decreased.

The temperature T_s at which the ZFC and the FC curves separate corresponds to the blocking of the largest particles, while the maximum of the ZFC curve (T_{max}) can be related to the blocking of particles with the average volume. T_s increases with the temperature of the thermal treatment and T_{max} moves from 6.0 K for Fe900 to 5.0 K for Fe700, while it falls below 2 K for the other samples. This trend is in agreement with the occurrence of smaller particles in the samples treated at lower temperatures, as shown by TEM.

The μ_{eff} values measured at 70 K vary from about 2.8 μ_B for samples treated up to 700 °C, to 14 μ_B for the Fe900 specimen. The former value is much lower than

(18) Morrish, A. H. *The Physical Principles of Magnetism*; John Wiley and Sons: New York, 1965.

expected for noninteracting iron(III) ions (5.9 μ_B), while the latter is much higher, thus indicating that the formation of a ferrimagnetic phase, corresponding to γ-Fe_2O_3 particles, occurs only between 700 and 900 °C.

An evaluation of the average magnetic volume of the particles of the Fe900 sample was made from the high field dependence of the magnetization.[19] From the fit of the data collected at different temperatures up to 7 T, an average diameter of 3.8 nm was obtained. The relatively small broadening of the ZFC curve and the closeness of T_s and T_{max} can be taken as a qualitative indication of a narrow size distribution, in agreement with TEM observations.

The dynamics of the relaxation of the magnetization were monitored with ac susceptibility experiments. According to the Néel theory,[20] the magnetic moment of noninteracting single-domain identical particles, with uniaxial anisotropy, fluctuates between the two directions of the easy axes with a relaxation time that follows an Arrhenius law:

$$\tau = \tau_0 \exp(KV/k_B T)$$

where k_B is Boltzmann's constant, T the absolute temperature, K the effective anisotropy energy constant, V the volume of the particle, and τ_0 is a preexponential factor which is of the order of $10^{-9}-10^{-11}$ s for ferro- and ferrimagnetic nanoparticles. Several effects contribute to the overall observed K, the most important being magnetocrystalline, surface, and shape anisotropy.

An evaluation of the average energy barrier KV and of the preexponential factor can be directly obtained by ac susceptibility experiments. In fact the temperature corresponding to the maximum of the in-phase component of the susceptibility can be identified with the blocking temperature, i.e., the temperature at which the relaxation time is equal to the time scale of the experiment τ_m which, in an ac susceptibility experiment is given by the reverse of the measuring frequency, $\tau_m = 1/\nu_{ac}$. The plot of $\ln(\tau_m)$ vs $1/T_{max}$ must then give a straight line with slope KV and intercept τ_0.

Data for Fe900 (Figure 5) show that, in the investigated range of frequencies, the sample follows an Arrhenius law, with $\tau_0 = 1 \times 10^{-10}$ s and $KV = 3.4 \times 10^{-21}$ J. By using the value of $\langle V \rangle$ measured from magnetization data, the average anisotropy constant $K = 1 \times 10^5$ J/m^3 was evaluated. This value is 2 orders of magnitude larger than that of the bulk, as usually observed for nanometric particles,[21] in which the surface and the shape contributions to the anisotropy are greatly increased.

EPR and FIMR. EPR experiments on Fe300 and Fe700 show spectra with two main signals located at $g \sim 2$ and $g \sim 4.3$; the result for Fe700 is shown in Figure 6. This kind of behavior has also been observed in other amorphous samples of $Fe_2O_3-SiO_2$.[12] The two signals can be assigned to two different Fe(III) sites: the $g \sim 2$ site is a normal bulk octahedral or tetrahedral site,

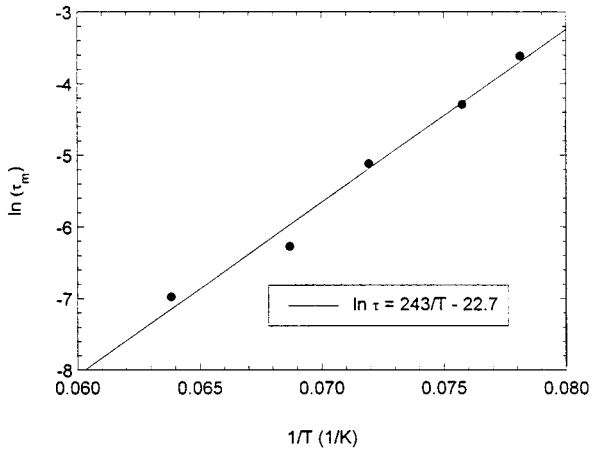

Figure 5. Temperature dependence of the relaxation time of the magnetization extimated from ac susceptibility data for the Fe900 sample. Experiments were made in the frequency range 36−1070 Hz.

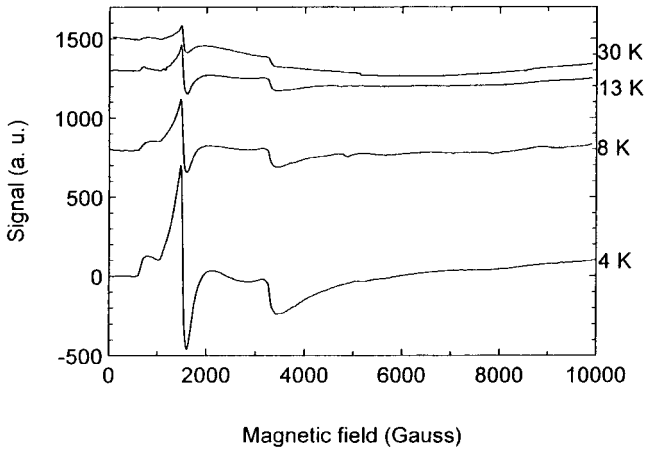

Figure 6. X-band EPR spectra of the Fe700 sample between 4 and 30 K.

whereas the $g \sim 4.3$ is a strongly distorted rhombic site that presumably is located on the surface of the particle, in contact with the SiO_2 matrix. The position of the two lines is constant in the whole temperature range, indicating the absence of an internal field and also of a blocked region.

In samples treated at higher temperature, another type of signal is observed, which is typical of ferrimagnetic resonance (FIMR) in small magnetic particles (Figure 7). Qualitatively, the temperature dependence of the absorption spectrum of magnetic particles in a magnetic resonance experiment can be understood according to the Raikher and Stepanov model.[22] Above the blocking temperature (T_B), the thermal fluctuation energy is larger than the uniaxial anisotropy energy ($k_B T > KV$), and so it smears out the influence of the anisotropy: the spectrum is just like a normal paramagnetic spectrum with a resonance at $h\nu = g\mu_B H$, g being an effective g factor depending on the peculiar system. Below the blocking temperature, the anisotropy energy is larger than the thermal fluctuations ($k_B T < KV$) and so the absorption will be smeared along the random distribution of the effective anisotropy field H_a (where $H_a = 2|K|/M$, M being the magnetization of the

(19) Djega-Mariadassou, C.; Dormann, J. L.; Nogués, M.; Villers, G.; Sayouri S. *IEEE Trans. Magn.* **1990,** *26*, 1819.
(20) Néel, L. *Ann. Geophys.* **1949**, *5*, 99.
(21) Tronc, E.; Prene, P.; Jolivet, J. P.; d'Orazio, F.; Lucari, F.; Fiorani, D.; Godinho, M.; Cherkaoui, R.; Nogues, M.; Dorman, J. L. *Hyperfine Interact.* **1995**, *95*, 129.
(22) Raikher, Y. L.; Stepanov, V. I. *Phys. Rev. B* **1994**, *50*, 6250.

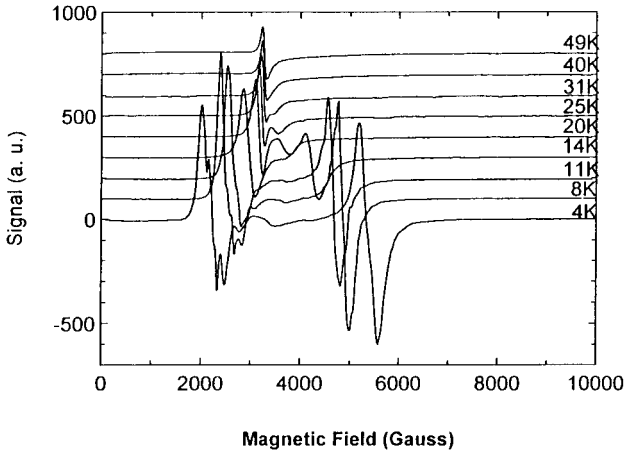

Figure 7. Temperature dependence of the X-band EPR spectra of the Fe900 sample between 4 and 49 K.

particles). When the anisotropy field is smaller than the Zeeman field ($H_a < H$), the two peaks of the typical absorption spectrum will be separated by $3|K|/M$ and placed at $+K/M$ and $-2K/M$ around the Zeeman field. In the case of a negative anisotropy constant, like the one in γ-Fe_2O_3, the high-field part will be placed at $H + 2|K|/M$ and the low-field resonance at $H - |K|/M$. This is clearly the observed behavior (Figure 7). The blocking temperature obtained by these experiments is in the region 30−40 K, and 40 K can be a good estimate. Compared to the other experimental techniques, the EPR gives a rather high T_B. This is due to the short time scale of the experiment ($\tau_m \sim 10^{-10}$ s). However, the use of an external magnetic field may reduce the blocking temperature by lowering the barrier for reorientation of the magnetization.

In fact, high-field EPR experiments (exciting frequency 250 GHz, magnetic field up to 12 T) were performed on the samples, and no blocking temperature was observed even with the sample Fe900. The very high exciting frequency should give rise to a blocking temperature about 30 times that measured at X-band, because the frequency is 30 times higher. But, at the same time, the Zeeman resonance field is increased with the same ratio. The absence of a blocking temperature shows that field dependence of the relaxation process is more important than the frequency one.

Theory provides also the dependence of the effective anisotropy field on temperature:[22] $H_a(T) = h_a(1/L(\xi) - 3/\xi)$, where h_a is the "true" anisotropic field, $\xi = MVH/k_BT$ and $L(\xi)$ is the Langevin function. This temperature dependence comes from the damping of the free precession of the magnetization around the Zeeman field in ordered magnetic compounds. Tentative fits were tried on the experimental data of $H_a(T)$ to find values of h_a and V; the obtained values are $h_a = 1450$ G and $V = 16.86$ nm^3 (using $H = 3300$ G and $M = 64$ G, i.e., the value of the magnetization under an applied field of 3300 G). From the mean volume of the particles, a mean diameter $d = 3.2$ nm was found; from h_a the value of the anisotropy constant, $|K| = 4.64 \times 10^5$ J/m^3 was obtained. Both values are in the same range as that found from magnetization relaxation measurements.

Mössbauer Spectroscopy. The Mössbauer absorption spectra of the Fe300, Fe500, Fe700, and Fe900 samples are shown in Figure 8, while Figure 9 shows

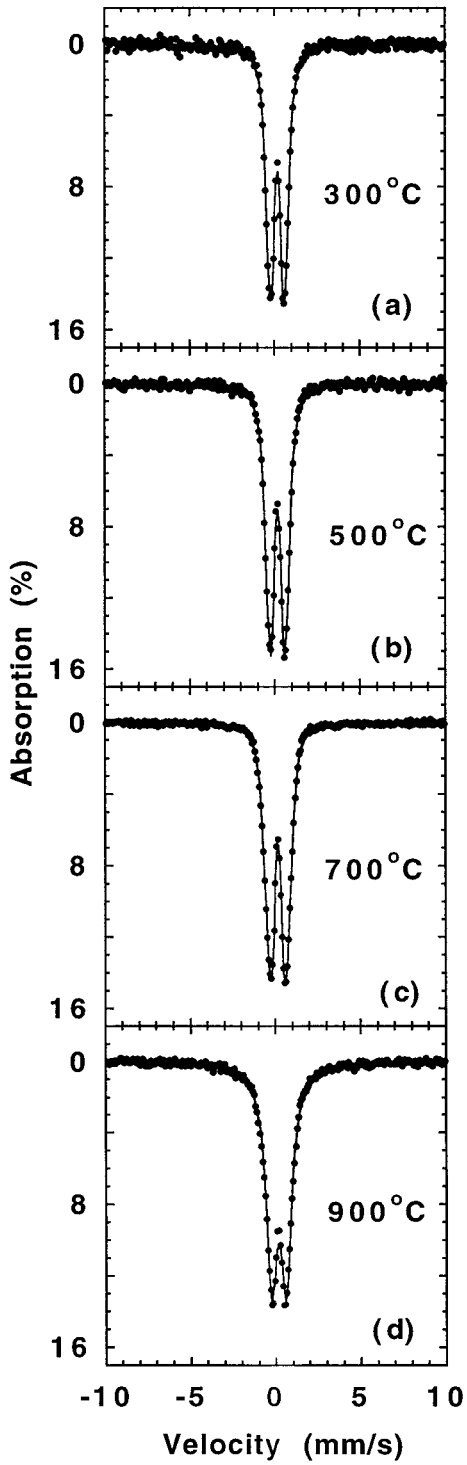

Figure 8. Mossbauer spectra (a−d) (dots) of the samples heat treated at the reported temperatures; simulated spectra (solid lines).

the spectrum of Fe1100. The samples treated up to 900 °C are in a paramagnetic state, while the Fe1100 sample is magnetically ordered.

The absorption spectra were simulated by peaks with Lorentzian shape. Actually, amorphous materials do not show simple Lorentzian line shapes, owing to the structural disorder; moreover the presence of phenomena of paramagnetic relaxation in the nanoparticles also changes the line shape.[23] Therefore this fitting procedure must be considered as an approximation. All the spectra were tentatively fitted by a single quadrupole

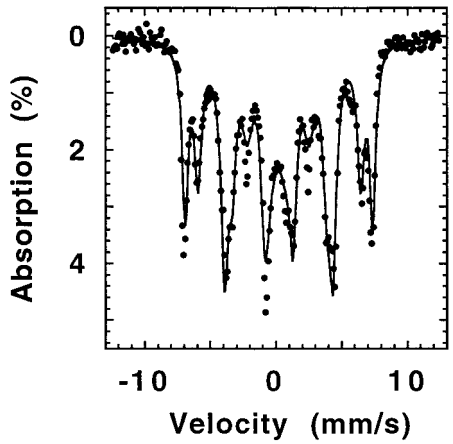

Figure 9. Mossbauer spectrum (dots) of the sample treated at 1100 °C; simulated spectrum (solid line).

Table 1. Mössbauer Parameters As Obtained by Fitting the Spectra of the Samples[a]

sample	component	δ (mm/s)	Δ (mm/s)	B (T)	Γ (mm/s)	area (%)
Fe300	1	0.29(1)	0.61(2)		0.36(2)	42
	II	0.28(1)	1.07(2)		0.48(2)	58
Fe500	I	0.28(1)	0.68(1)		0.39(1)	48
	II	0.28(1)	1.18(2)		0.48(1)	52
Fe700	I	0.28(1)	0.61(1)		0.36(1)	36
	II	0.28(1)	1.06(1)		0.41(1)	41
	III	0.26(1)	1.59(1)		0.46(1)	23
Fe900	I	0.28(1)	0.86(1)		0.78(1)	
Fe1100	I	0.36(1)			2.20(1)	12
	II	0.36(1)		44.4(1)	0.56(1)	32
	III	0.40(1)		38.5(1)	0.65(1)	28
	IV	0.31(1)		25.3(1)	0.93(1)	28

[a] Table shows the values of isomer shift (δ), quadrupole splitting (Δ), magnetic field (B), full width at half-maximum of the peaks (Γ) and absorption of each component (area). The standard deviation of the parameters is given in parentheses as uncertainty on the last digit.

doublet with free parameters, using a least-squares method. The introduction of further doublets gave rise to improvements of the fits which were considered significant only when the χ^2 parameter was reduced more than 10%. The χ^2 value for the fits reported was about 2.

The values of isomer shift IS (δ), quadrupole splitting QS (Δ), internal magnetic field (B), and full width at half-maximum fwhm (Γ) resulting from the best fits are reported in Table 1. The contribution of each component to the total absorption area (A) is also given. All the spectra show components with values of IS typical of trivalent iron.[24,25]

The Fe300 and Fe500 spectra (Figure 8) were fitted by two quadrupole doublets, which have the same IS but very different QS. The component with smaller QS corresponds to internal iron sites, while the other is due to the ones on the surface of nanoparticles; the bigger QS of the second component is explained with the higher distortion of the superficial iron sites. The area ratio of components I and II increases from Fe300 to Fe500, according to the increase of the volume/surface ratio with the particle size, as revealed by TEM and XRD. These results are also in agreement with EPR data.

The spectrum of the Fe700 sample was fitted by three Lorentzian doublets. The components I and II have IS and QS close to those of the Fe300 and Fe500 samples. The third component has a very different QS; it can be assigned to a newly formed phase, which probably gives also a contribution to components I and II. The appearance of this new component coincides with the appearance of the peaks of the γ-phase in the XRD data.

The absorption peaks of the Fe300, Fe500, and Fe700 samples are broadened with respect to those of a crystalline material, with fwhm values similar to those found for Fe(III) in glasses; this broadening can be explained as an effect of structural disorder.[26,27]

The spectrum of the Fe900 sample can be simulated by a single doublet, which has a much larger fwhm than that of the samples treated up to 700 °C; this fact hides the complex structure of the spectrum found in the other samples. The fwhm found ($\Gamma = 0.78$ mm/s) cannot be due to structural disorder; it is due to paramagnetic relaxation-related phenomena.[23] The relaxation time depends on the magnetization of the material and is larger in ferrimagnetic than in antiferromagnetic materials;[20,28−30] on the other hand, in the paramagnetic state the peak width increases with relaxation time.[23] Therefore this change of the peak widths from Fe700 to Fe900 is in agreement with the large increase of magnetization, revealed by magnetic measurements.

The spectrum of the Fe1100 sample was fitted by three magnetic sextuplets and one singlet (Figure 9). The lines due to the magnetic structure have fwhm values equal to 2−4 times the typical crystalline width, while the singlet is much larger. The sextuplets indicate the presence of magnetic order in the sample, while the singlet takes into account the nonordered particles.[21,30] The three components have magnetic fields smaller than those of the corresponding bulk phases, because of the nanocrystalline character of the particles;[29] in particular, fields of about 44 T were found in nanoparticles of ferric oxide in silica.[7,13] Therefore, it is impossible to assign the single components to precise phases. Three phases are however indicated. Two of the ordered components are due to the γ- and α-phases, evidenced by XRD data. The third component could be due to another quite rare oxide phase, ϵ-Fe_2O_3, which has been already observed in similar $Fe_2O_3-SiO_2$ composites submitted to analogous thermal treatments.[6] This phase gives rise to XRD reflections similar to those of γ- and α-phases, so that they might be hindered under the complex Fe1100 XRD spectrum.

Discussion

The preparation route here reported has been successful in providing nanoparticles, in which the iron is present exclusively as Fe(III). The particle size slightly increases in the samples treated at high temperature but retains a narrow distribution. However, all the

(23) Wickman, H. H. *Mössbauer Effect Methodology*; Gruverman, I. J., Ed.; Plenum Press: New York, 1966; Vol. 2, p 39.
(24) Gutlich, P.; Link, R.; Trautwein, A. *Mössbauer Spectroscopy and Transition Metal Chemistry*; Springer-Verlag: Berlin, 1978; p 56.
(25) Darby Dyar, M. *Am. Mineral.* **1985**, *70*, 304.
(26) Concas, G.; Congiu, F.; Muntoni, C.; Pinna, G. *J. Phys. Chem. Solids* **1995**, *56*, 877.
(27) Kurkjan, C. R.; Sigety E. A. *Phys Chem. Glasses* **1968**, *9*, 73.
(28) Brown, W. F. Jr. *Phys. Rev.* **1963**, *130*, 1677.
(29) Mørup, S.; Topsoe, H.; Lipka, J. *J. Phys.* **1976**, *35*, C6−207.
(30) Tronc E. *Nuovo Cimento D* **1996**, *18*, 163.

observations indicate that the nature of the particles change with thermal treatment.

On heating the dried gels, particles first formed from the decomposition of iron nitrate are X-ray amorphous. This can be the result either of a very disordered structure or of a crystallite size so small as to escape observation by XRD. The amorphous structure of the particles is confirmed by dark-field TEM images, which show only a very small number of crystalline nanoparticles, in agreement with literature information. Ayyub et al.[31] synthesized micrometric particles of Fe_2O_3 having different sizes by a microemulsion technique. They observed a succession of size-induced structural transformations. In particular, when the particle size falls below ∼5 nm, the XRD data become like those of a completely amorphous sample, while crystallites of this size would give rise to a small number of broad XRD lines. Van Diepen and Popma[32] prepared, by thermal decomposition of an aerosol containing iron(III) chloride, an X-ray amorphous Fe_2O_3 form, for which magnetic susceptibility measurements indicated an antiferromagnetic clustering in an aperiodic structure. These two observations can account for the antiferromagnetic susceptibility values reported in the present paper for the samples treated at $T < 800$ °C.

In this condition the particles certainly have a great number of iron atoms at their surface, which are likely to interact with the silica network. This consideration accounts for both the EPR and Mössbauer data, which suggest the presence of two sites for Fe(III) in the samples treated at low temperature.

Further heating leads to a progressive disentanglement of the small iron oxide clusters from the SiO_2 support. At high temperature, the mobility of the ions can be sufficient to cause particle coalescence and growth. Disordered particles can still be present, but they are gradually substituted by more ordered clusters. As a consequence, a great number of nanocrystallites of γ-Fe_2O_3 is observed in TEM micrographs and the γ-Fe_2O_3 peaks become increasingly evident in the XRD data. At the same time, the susceptibility values exhibit superparamagnetic behavior but indicate the formation of a ferrimagnetic phase, the number of Fe(III) atoms at the surface of particles or in distorted sites decrease, a ferrimagnetic resonance appears in the EPR spectra and a ferrimagnetic effect is shown by the variation of Mössbauer signals.

All these observations suggest a strong interaction between the iron atoms and the SiO_2 network in the samples treated at low temperatures. In fact, the formation of an α-Fe_2O_3 phase occurs at higher temperatures than in pure or weakly interacting Fe_2O_3 particles. Similar behavior has been observed in other supported metal oxides[33,34] (besides Fe_2O_3 deposited on SiO_2[7]) and has always been considered as an indication of a chemical interaction between metal atoms and a matrix. Spectroscopic investigations about this problem are in progress. Indirect evidence of this hypothesis is given by the fact that the iron ions are strongly resistant

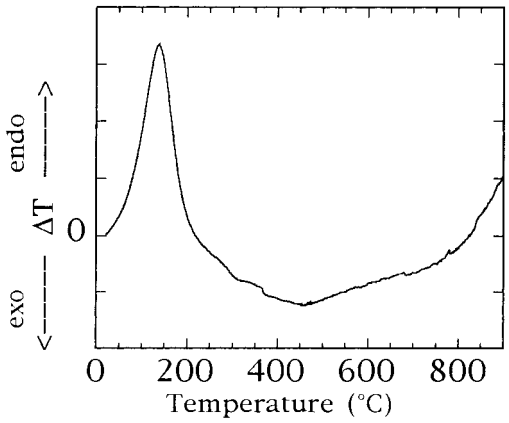

Figure 10. DTA trace of the Fe300 sample.

to reduction treatments. In fact, fluxing the Fe300 sample with H_2 for 2 h at 600 °C gives rise to a small amount of Fe(II) silicate phase, but the formation of metallic iron is not detected either by XRD or by Mössbauer spectroscopy. Particle−support interactions might involve either the presence of Fe−O−Si bridges at the interface of the two oxides or the replacement of tetrahedral Fe(III) sites in the iron oxide phase by Si(IV).[7,13] The formation of some chemical compound could also be invoked, though it does not seem realistic. In fact, the formation of γ-Fe_2O_3 from some silicate precursor would take place with important structural modifications, which are not suggested by XRD and TEM.

This is confirmed by DTA measurements (Figure 10) that, besides an endothermic peak at low temperature due to water elimination, show a broad exothermic signal spread over 600 °C, which suggests a continuous transition from amorphous to crystalline phase. In this temperature range, XRD reveals the beginning of the α-Fe_2O_3 formation. Also the transition γ- to α-Fe_2O_3 gives an exothermic DTA trace,[31] that in the present case is superimposed on the amorphous to γ-Fe_2O_3 transition trace.

The observed behavior suggests that iron oxide particles are not present in a unique form. The low-temperature treatments determine the prevalence of amorphous particles, but the presence of a nonnegligible amount of maghemite cannot be ruled out. Higher temperature treatments lead to an increase of γ-Fe_2O_3 particles, which form the dominant phase at 900 °C, then the α-Fe_2O_3 phase begins to form. This slow and continuous transition could in part explain why the changes in the system induced by heating are revealed by different techniques after different thermal treatments. In particular, XRD and Mössbauer give evidence of γ-Fe_2O_3 formation in the Fe700 sample, for which EPR and magnetic susceptibility observations do not display meaningful transformation. This may depend on the different sensitivity of these techniques to structural modifications, since they react to different aspects of these modifications (local order, long-range order, surface phenomena). This hypothesis is reliable since the transitions described are the result of a series of complicated phenomena. For instance, when the original amorphous particles separate from the support and γ-Fe_2O_3 begins to form, the distribution of the cations in the vacancies of the spinel structure of

(31) Clause, O.; Bonneviot, L.; Che, M. *J. Catal.* **1992**, *138*, 195.
(32) Zielinski, J. *Catal. Lett.* **1995**, *31*, 47.
(33) Ayyub, P.; Multani, M.; Barma, M.; Polkar, V. R.; Vijayaraghavan, R. *J. Phys. C: Solid State Phys.* **1988**, *21*, 2229.
(34) Van Diepen, A. M.; Popma, Th. J. A., *J. Phys.* **1976**, *C-6*, 755.

maghemite changes with particle size.[35] The same lattice parameters change as a function of particle size.[31] Therefore, particles with the habitus of γ-Fe_2O_3, but in which magnetic order is hindered, can grow. According to this hypothesis, the lack of full alignment of the spins in ultrafine particles (~7.5 nm) was demonstrated long ago by Coey[36] and was recently[37] explained as an effect of canting of individual spins either in the surface or in the bulk of magnetic particles. Obviously, a well-grounded interpretation of the observed phenomena requires further investigation on a larger series of samples. In particular, changing the amount of iron atoms and/or some details of the preparation route will help on one hand to clarify the real nature of iron-containing particles and on the other hand to find ways of obtaining exclusively nanoparticles of γ-Fe_2O_3.

Conclusions

A $Fe_2O_3-SiO_2$ nanocomposite was prepared by a gelation method which uses tetraethoxysilane and iron-(III) nitrate as starting materials. The nature of the particles changes when samples are subjected to thermal treatments at elevated temperatures. In fact, the XRD patterns are completely amorphous for samples treated up to 600 °C, while at higher temperatures the formation of crystalline iron oxide phases is clearly observed. The transition from amorphous to crystalline particles is indicated also by TEM dark-field images. On the other hand, magnetic measurements show the transition from antiferromagnetic to ferrimagnetic susceptibility values, whereas Mössbauer and EPR spectral parameters exhibit clear qualitative variations that are connected to differences in sites and phases for Fe(III) ions. Maghemite is the predominant phase in the Fe900 sample.

Acknowledgment. Thanks are due to A. L. Barra (Laboratoire des Champs Magnetiques Intense, CNRS, Grenoble) for performing the high-frequency EPR spectra and to Prof. C. Muntoni (Dipartimento di Scienze Fisiche, Cagliari) for helpful suggestions. This work has been supported by CNR Grant 95.01588 CT 11.

CM970400U

(35) Haneda, K.; Morrish, A. H. *Solid State Commun.* **1977,** *22*, 779.
(36) Coey, J. M. D. *Phys Rev. Lett.* **1971**, *27*, 1140.
(37) Linderoth, S.; Hendriksen, P. V.; Bødker, F.; Wells, S.; Davies, K.; Charles, S. W.; Mørup, S. *J. Appl. Phys.* **1994**, *75*, 6583.